First occurrence of iodine in natural sulfosalts: The case of mutnovskite, Pb$_2$AsS$_3$(I,Cl,Br), a new mineral from the Mutnovsky volcano, Kamchatka Peninsula, Russian Federation

MICHAEL ZELENSKI,[1] TONČI BALIĆ-ŽUNIĆ,[2] LUCA BINDI,[3] ANNA GARAVELLI,[4] EMIL MAKOVICKY,[2] DANIELA PINTO,[4] AND FILIPPO VURRO[4],*

[1]Institute of Volcanology, Russian Academy of Sciences, Bulvar Piipa 9, Petropavlovsk-Kamchatsky, 683006 Russia
[2]Geological Institute, University of Copenhagen, Øster Voldgade 10, DK-1350 Copenhagen K, Denmark
[3]Museo di Storia Naturale, Sezione di Mineralogia, Università degli Studi di Firenze, Via La Pira, 4-I-50121 Firenze, Italy
[4]Dipartimento Geomineralogico, Università degli Studi di Bari, Via E. Orabona 4, I-70125 Bari, Italy

ABSTRACT

Mutnovskite, ideally Pb$_2$AsS$_3$(I,Cl,Br), is a new mineral from the high-temperature fumaroles of the Mutnovsky volcano, Kamchatka Peninsula, Russian Federation. It occurs as microscopic ruby-colored short-prismatic crystals up to 100 μm across, closely associated with halogen-sulfosalts of Pb, Bi, and As, Cd-Pb-Bi sulfosalts, pyrite, anhydrite, and cristobalite. Mutnovskite is transparent in thin fragments with a dark-red to blue color. The crystals are soft and fragile. Cleavage and fracture were not observed and the Mohs hardness is approximately 2. In reflected light mutnovskite is silvery lead-grey in color with an iridescent tarnish. Pleochroism and anisotropy are not visible because of the strong orange internal reflections, especially in immersion. Reflectance percentages measured in air in the range 400–700 nm were tabulated. Reflectance percentages (R_{min} and R_{max}) for the four COM wavelengths are 34.2, 34.6 (470 nm), 33.2, 33.5 (546 nm), 32.5, 32.7 (589 nm), and 31.4, 31.7 (650 nm), respectively. A mean of four electron microprobe analyses gave Pb 62.0(3), As 11.0(4), Bi 0.6(1), S 14.4(2), Se 0.2(3), I 8.9(3), Cl 2.44(9), Br 1.1(7), Cu 0.03(2), Fe 0.01(1), total 100.7 wt%, corresponding, on the basis of a total of 7 atoms, to Pb$_{1.99}$(As$_{0.98}$Bi$_{0.02}$)$_{\Sigma1.00}$(S$_{2.98}$Se$_{0.02}$)$_{\Sigma3.00}$(I$_{0.47}$Cl$_{0.46}$Br$_{0.09}$)$_{\Sigma1.02}$. The nine strongest powder-diffraction lines [d in Å (I/I_0) (hkl)] are: 4.69 (32) (002); 4.37 (67) (210); 3.34 (73) (020); 3.19 (100) (212); 2.715 (61) (022); 2.648 (66) (410); 2.539 (31) (213); 2.455 (29) (402); 1.894 (30) (232). Mutnovskite is orthorhombic, space group *Pnma*, with a = 11.543(1), b = 6.6764(7), and c = 9.359(1) Å, V = 721.3(1) Å^3, Z = 4. The crystal structure was solved and refined to R = 4.14%. It consists of three independent cation positions: Pb1 and Pb2 have tricapped trigonal prismatic coordinations with S and I atoms (completed with one As atom in the case of Pb2), while As has threefold coordination with S atoms, which form the base of a trigonal pyramid with As at the apex. Pairs of Pb1-Pb2 prisms are connected in columns which extend along **c**. AsS$_3$ coordinations are isolated from each other. S atoms and half of the Pb atoms form wavy close-packed layers. Two kinds of channels parallel to **b** occur between the layers. The smaller channels host As atoms close to the channel walls, with their lone-electron pairs occupying the median part, while the bigger ones accommodate rows of alternating halogen and Pb atoms. The new mineral is named after the type locality, the Mutnovsky volcano, Kamchatka Peninsula, Russian Federation.

Keywords: Mutnovskite, chemical composition, new mineral, X-ray data, crystal struture, Kamchatka Peninsula, Mutnovsky volcano

INTRODUCTION

The new mineral described herein, mutnovskite, Pb$_2$AsS$_3$(I,Cl,Br), is an unusual mineral species from high temperature fumaroles at the Mutnovsky volcano (Kamchatka Peninsula, Russian Federation), an interesting, and up to now scarcely investigated source of rare sublimate minerals. Mutnovskite represents the first iodine-bearing sulfosalt occurrence reported in nature. According to both the chemical composition and X-ray powder data, the mineral has no analogues among minerals or synthetic compounds. With the exception of the halogen content, however, the chemical composition is close to the recently approved mineral tsugaruite, Pb$_4$As$_2$S$_7$ (Shimizu et al. 1998).

The name mutnovskite is for the type locality. The type material is housed in the mineralogical collection of the Museum "C.L. Garavelli", Dipartimento Geomineralogico, Università di Bari, under the catalogue number 7/nm (V28). The polished sections used for both the quantitative reflectance and electron-microprobe studies, as well as the crystal of mutnovskite used for the structural study, are preserved at the Dipartimento Geomineralogico, Università di Bari. The mineral and mineral name have been approved by the IMA Commission on New Minerals and Mineral Names (2004-032).

OCCURRENCE AND ASSOCIATED MINERALS

Mutnovskite was found among volcanic sublimates at the Mutnovsky volcano, southern Kamchatka, Russia (52.35° N, 158.27° E) at a temperature of about 250 °C. It occurs as microscopic ruby to brownish-red euhedral crystals up to 100 μm

* E-mail: f.vurro@geomin.uniba.it

across, directly deposited on the host rock (Fig. 1), as well as on other Pb-Bi-As sulfosalts previously grown. The mutnovskite crystals exhibit a short-prismatic morphology, sometimes tabular, and are without inclusions or intergrowths with other minerals. In the samples analyzed, mutnovskite is closely associated with the Cd-bearing Pb-Bi sulfosalts, kudriavite, and Cd-cannizzarite, but especially with needle-like crystals of less-characterized Pb-Bi-As sulfosalts currently under study. Other minerals spatially associated with mutnovskite are sulfohalides and halogen-sulfosalts of Pb, Bi, and As, pyrite, anhydrite, and cristobalite. A complete description of the geological setting of the fumarole deposit from which mutnovskite was collected is given by Zelenski and Bortnikova (2005).

OPTICAL AND PHYSICAL PROPERTIES

Mutnovskite is transparent in thin fragments with a dark-red to blue color. It has a cherry-red to orange streak and the luster is resinous to submetallic.

In reflected light mutnovskite is silvery lead-gray in color with an iridescent tarnish. Pleochroism and anisotropy are not visible owing to the strong orange internal reflections, especially in immersion oil.

Reflectance measurements were performed in air by means of a MPM-200 Zeiss microphotometer equipped with a MSP-20 system processor on a Zeiss Axioplan ore microscope. The filament temperature was approximately 3350 K. Readings were taken for specimen and standard (SiC) maintained under the same focus conditions. The diameter of the measuring area was 0.1 mm. Reflectance percentages for R_{min} and R_{max} in the range 400–700 nm in 20 nm increments are reported in Table 1. In Figure 2 the reflectance percentages for mutnovskite together with those measured by Shimizu et al. (1998) for tsugaruite, $Pb_4As_2S_7$, are plotted. The reflectance values for the two minerals are almost identical, which shows the necessity of a chemical analysis or diffraction study to distinguish between them.

The mutnovskite crystals are soft and fragile. Cleavage and fracture were not observed and the Mohs hardness is approximately 2. The density could not be measured owing to the dearth of material and the small size of the crystals. The calcu-

lated density, obtained from the chemical formula and unit-cell parameters, is 6.177 g/cm^3. Twinning was not observed in the morphological characteristics of crystals or in their optical properties. In addition, no indications of twinning were discovered during the X-ray diffraction study.

CHEMICAL COMPOSITION

Four crystal fragments of mutnovskite were analyzed with a Jeol JXA-8600 electron microprobe at the Dipartimento di Scienze della Terra, Università di Firenze. The operating conditions were: accelerating voltage 15 kV, beam current 20 nA; standards (element, *emission line*, counting time for one spot analysis): galena (Pb$M\alpha$, 20 s); marcasite (Fe$K\alpha$, 40 s; S$K\alpha$, 20 s); iodargyrite (I$L\alpha$, 20 s); tugtupite (Cl$K\alpha$, 20 s); synthetic GaAs (As second order $L\alpha$, 40 s); synthetic Bi$_2$Se$_3$ (Bi$M\alpha$, 40 s; Se second order $L\alpha$, 40 s), covellite (Cu$K\alpha$, 40 s), pure Tl (Tl$M\alpha$, 40 s), and bromargyrite (Br second order $L\alpha$, 40 s). The estimated analytical precision (in wt%) is: ± 0.60 for Pb, ± 0.50 for I; ± 0.30 for Bi, Cl, and Br; ± 0.20 for As and S; ± 0.10 for Se; ± 0.05 for Fe, Cu, and Tl. The results of the analysis, the average chemical composition and the theoretical composition in wt% of elements, are reported in Table 2. The valence balance is rather good: deviations do not exceed about 2.9% in absolute value. Mutnovskite clearly contains minor Bi [up to 0.02 atoms per formula unit (apfu)], Se (up to 0.11 apfu), and Br (up to 0.17 apfu) in addition to the major constituents Pb (1.94 to 2.01 apfu), As (0.94 to 1.01 apfu), S (2.93 to 3.01 apfu), Cl (0.44 to

TABLE 1. Reflectance measurements in air for mutnovskite

λ (nm)	R_{min} (%)	R_{max} (%)	λ (nm)	R_{min} (%)	R_{max} (%)
400	39.2	44.1	560	32.9	33.1
420	38.6	39.4	580	32.7	32.8
440	36.5	37.6	**589**	**32.5**	**32.7**
460	35.3	36.2	600	32.2	32.5
470	**34.2**	**34.6**	620	31.9	32.1
480	33.9	34.2	640	31.7	31.9
500	33.7	34.0	**650**	**31.4**	**31.7**
520	33.6	33.8	660	31.2	31.4
540	33.4	33.6	680	30.9	31.0
546	**33.2**	**33.5**	700	30.7	30.8

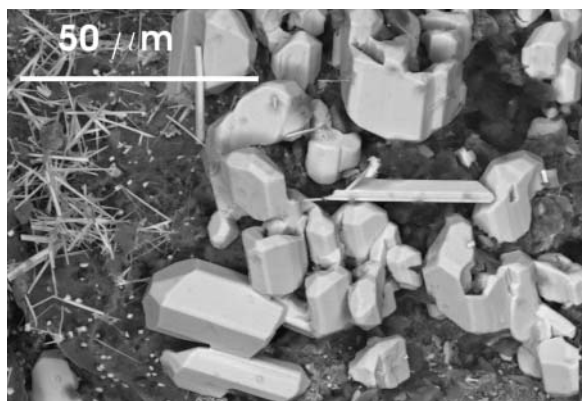*Note:* The four COM wavelengths at 470, 546, 589, and 650 are indicated in bold.

FIGURE 1. Scanning electron photomicrograph of mutnovskite crystals (BSE image). Needle-like crystals of Pb-Bi-As halogen-sulfosalts, which are currently under study, appear on the left.
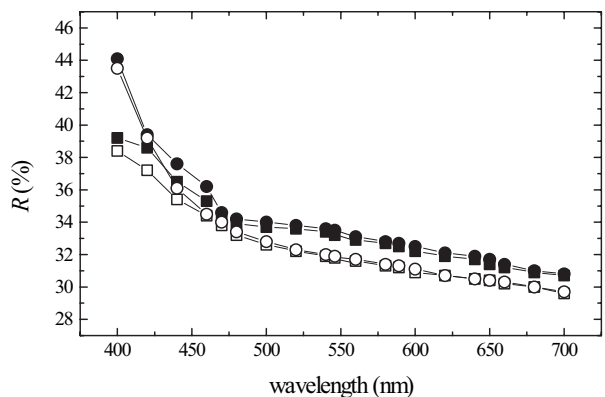

FIGURE 2. Reflectivity curves for mutnovskite in air. Open symbols refer to tsugaruite (Shimizu et al. 1998), filled symbols refer to mutnovskite (this study). Circles and squares refer to R_{max} and R_{min} values, respectively.

TABLE 2. Chemical composition of mutnovskite (microprobe data, wt%) and empirical chemical formulas

No.	Pb	Fe	Cu	Bi	As	S	Se	Cl	I	Br	Total	Val. %*
1	61.40	0.02	–	0.51	10.54	14.22	-	2.62	9.06	1.61	99.98	2.83
2	61.02	–	0.02	0.53	11.28	14.49	0.70	2.41	9.04	1.37	100.86	2.73
3	61.65	0.03	0.01	0.58	10.81	14.31	0.55	2.45	8.86	0.06	99.31	0.84
4	62.40	–	0.01	0.45	10.63	14.24	0.38	2.44	8.90	2.06	101.51	2.65
5	62.07	–	0.07	0.47	11.03	14.31	1.33	2.63	8.32	0.93	101.16	2.70
6	61.84	0.01	0.04	0.70	11.59	14.59	–	2.53	8.72	1.86	101.88	0.14
7	61.94	-	0.02	0.55	11.04	14.31	–	2.48	8.69	1.21	100.28†	0.24
8	62.37	0.01	0.04	0.47	10.80	14.18	0.33	2.31	9.39	1.05	100.95	0.29
Average‡	61.95	0.01	0.03	0.58	11.06	14.35	0.22	2.44	8.92	1.05	100.61	1.50
Theoretical§	62.15	–	–	–	–	11.24	14.43	–	2.66	9.52	–	100.00

* Valence in % was calculated with formula : $|\,[\sum(\text{val}^+) - \sum(\text{val}^-)] \times 100/\sum(\text{val}^-)\,|$.
† Includes 0.04 wt% Tl.
‡ Calculated from four selected analyses (No. 3, 6, 7, 8) with a good balance of valence (deviations less than 1.5%).
§ Calculated from the ideal formula : $Pb_2AsS_3(I,Cl)$.

Empirical chemical formulas of selected analyses (based on 7 apfu):
3. $Pb_{2.00}(As_{0.97}Bi_{0.02})_{\Sigma0.99}(S_{3.01}Se_{0.05})_{\Sigma3.06}(I_{0.47}Cl_{0.47}Br_{0.01})_{\Sigma0.95}$
6. $Pb_{1.96}(As_{1.01}Bi_{0.02})_{\Sigma1.03}S_{2.99}(I_{0.45}Cl_{0.47}Br_{0.15})_{\Sigma1.07}$
7. $Pb_{2.00}(As_{0.98}Bi_{0.02})_{\Sigma1.00}S_{2.98}(I_{0.46}Cl_{0.47}Br_{0.10})_{\Sigma1.03}$
8. $Pb_{2.01}(As_{0.96}Bi_{0.02})_{\Sigma1.00}(S_{2.96}Se_{0.03})_{\Sigma2.99}(I_{0.50}Cl_{0.44}Br_{0.09})_{\Sigma1.03}$

Average empirical formula
$Pb_{1.99}(As_{0.98}Bi_{0.02})_{\Sigma1.00}(S_{2.98}Se_{0.02})_{\Sigma3.00}(I_{0.47}Cl_{0.46}Br_{0.09})_{\Sigma1.02}$

0.49 apfu), and I (0.43 to 0.49 apfu). Traces of Fe, Cu, and Tl were also detected. With a total of 7 apfu, as determined from the crystal structure solution, the empirical chemical formulas for the best four determinations (balance of valence less than 1.5% in absolute value) were calculated and are reported in Table 2. The resulting average empirical formula for mutnovskite is $Pb_{1.99}(As_{0.98}Bi_{0.02})_{\Sigma=1.00}(S_{2.98}Se_{0.02})_{\Sigma=3.00}(I_{0.47}Cl_{0.46}Br_{0.09})_{\Sigma=1.02}$, very close to the ideal $Pb_2AsS_3(I,Cl,Br)$.

X-RAY DIFFRACTION STUDY

X-ray powder diffraction

The X-ray powder pattern for the holotype (Table 3) was obtained using a 57.3 mm Debye-Sherrer camera (Fe$K\alpha$). Indexing of the reflections was performed on the basis of the structure refinement, taking into account the calculated intensities. The following orthorhombic unit-cell parameters were obtained by least squares refinement: $a = 11.544(4)$, $b = 6.669(2)$, and $c = 9.365(4)$ Å.

Structural determination and refinement

A small crystal fragment ($34 \times 54 \times 72$ µm) was selected for X-ray single-crystal diffraction study. The X-ray data were collected using a Bruker AXS four-circle diffractometer equipped with a CCD SMART1000 area detector and flat graphite monochromator using Mo$K\alpha$ radiation from a fine-focus sealed X-ray tube (Table 4). SMART (Bruker AXS 1998) software was used to determine the orientation of the crystal lattice and for data collection; SAINT Plus (Bruker AXS 1997a) was used to integrate intensities and for Lorentz-polarization correction and calculation of the final unit-cell parameters. For the empirical absorption correction (ellipsoid approximation) the program XPREP from SHELXTL package (Bruker AXS 1997b) was used. The R_{int} factor after the empirical absorption correction was 6.92% compared to 12.47% before the absorption correction. The minimum and maximum X-ray transmission factors were 0.00901 and 0.04252, respectively.

Systematic absences ($0kl$: $k + l = 2n$; $hk0$: $h = 2n$; $h00$: $h = 2n$; $0k0$: $k = 2n$; $00l$: $l = 2n$) were consistent with space groups $Pn2_1a$ and $Pnma$. Statistical tests on the distribution of $|E|$ values strongly indicated the presence of an inversion center, thus suggesting the choice of space group $Pnma$.

The crystal structure of mutnovskite was solved by direct methods using the program SHELXS-97 (Sheldrick 1997a) and the subsequent structure refinement proceeded by means of the full-matrix least-squares program SHELXL-97 (Sheldrick 1997b). Neutral scattering factors for Pb, As, I, Cl, and S were taken from the *International Tables for X-ray Crystallography* (Ibers and Hamilton 1974). The solution revealed three cation sites. The As1 position was defined on the basis of its threefold coordination and bond lengths, which were characteristic for As^{3+} in

TABLE 3. X-ray powder-diffraction data for mutnovskite

I/I_o	d(obs)	d(calc)	h	k	l
5	5.770	5.772	2	0	0
7	5.440	5.433	0	1	1
7	4.930	4.914	2	0	1
32	**4.690**	**4.682**	**0**	**0**	**2**
67	**4.370**	**4.365**	**2**	**1**	**0**
12	3.970	3.956	2	1	1
12	3.620	3.636	2	0	2
73	**3.340**	**3.335**	**0**	**2**	**0**
100	**3.190**	**3.193**	**2**	**1**	**2**
10	2.890	2.886	4	0	0
19	2.763	2.746	2	0	3
61	**2.715**	**2.716**	**0**	**2**	**2**
66	**2.648**	**2.649**	**4**	**1**	**0**
31	**2.539**	**2.539**	**2**	**1**	**3**
29	**2.455**	**2.457**	**4**	**0**	**2**
26	2.294	2.294	1	0	4
5	2.234	2.236	1	2	3
22	2.180	2.182	4	2	0
22	2.123	2.125	4	2	1
16	1.976	1.978	4	2	2
19	1.914	1.916	3	1	4
30	**1.894**	**1.897**	**2**	**3**	**2**
11	1.849	1.849	6	1	0
15	1.814	1.814	6	1	1
15	1.780	1.780	3	3	2
13	1.760	1.761	4	3	0
10	1.730	1.728	2	3	3
8	1.715	1.715	3	2	4
11	1.666	1.667	0	4	0
18	1.634	1.633	3	1	5
13	1.621	1.622	5	2	3
9	1.589	1.591	6	1	3
15	1.572	1.571	0	4	2
5	1.505	1.507	1	1	6
6	1.474	1.474	5	2	4
7	1.455	1.454	3	4	2
17	1.425	1.425	7	1	3
15	1.395	1.395	8	1	1
6	1.380	1.380	4	4	2
10	1.335	1.333	5	2	5

sulfosalts. One anion site (X) showed an electron density higher than that of sulfur. This site was refined as a mixed (I,Cl) position giving occupancies of 0.52 for I and 0.48 for Cl. This corresponds to a mean number of electrons of 35.7, which is in excellent agreement with the value obtained from the chemical data (35.9). Br was not considered at the X site because of a very low content of this element relative to the accuracy of the method. However, as the refinement suggested that I and Cl

occupy the same site in the structure, it is most probable that a significant amount of Br can also enter, or even dominate at this site. As shown by the chemical analysis, the mutnovskite samples contain only low amounts of Br, but this is evidently due to the chemistry of the environment, and not to structural limitations. All attempts to refine the occupancy of the Pb sites (Pb + As), the As site (As + Bi), and the S sites (S + Se) produced values consistent with pure Pb, As, and S respectively. Attempts to refine the coordinates of I and Cl in the X site independently from each other resulted in an unstable refinement, and were abandoned.

The final refinement was performed with anisotropic temperature factors for all the atoms. The refinement of the crystal structure of mutnovskite converged to $R = 4.14\%$ for 753 observed reflections $[F_o > 4\sigma(F_o)]$ and $R = 5.63\%$ for all 976 independent reflections.

Inspection of the difference Fourier map revealed maximum positive and negative peaks of 2.04 and 3.23 e$^-$/Å^3, respectively. Crystal data, as well as details about data collection and refinement, are summarized in Table 4. Fractional atomic coordinates and anisotropic-displacement parameters are shown in Table 5. Table 6[1] lists the observed and calculated structure factors, while selected bond distances and angles are shown in Table 7.

As the atomic displacement ellipsoid of Pb2 was more anisotropic than for other structural sites (elongated along [010]), and the sum of valences for this site was significantly lower than the expected value of 2 (see Table 8), a refinement with Pb2 moved out of the symmetry plane was attempted (split-Pb2 site). The displacement factor had to be kept isotropic in this case to avoid large correlation factors.

The results showed splitting of the Pb2 site with a distance of 0.38 Å between the two possible positions on the two sides of the mirror plane. At the same time the R factors were worse than for the non-split refinement ($R1 = 4.89\%$), and the sum of the valences for the site did not improve significantly (1.77). It is interesting to note that, if the bonding between Pb2 and the neighboring As atom is included in the valence calculation, the sum for the Pb2 valence would be 1.91 (not-split) and 1.95 (split) respectively. As described later, the As atom completes the coordination of Pb2 as the "missing vertex" of the trigonal prism, and this can explain the lower sum of valences if it is excluded. Because no significant improvement in the reliability factors or the crystal-chemical parameters is obtained with the "split-refinement" and no evidence for the movement of Pb2 out of the mirror plane could be obtained, the results of the former refinement were accepted as final.

DESCRIPTION OF THE CRYSTAL STRUCTURE

In the crystal structure of mutnovskite (Fig. 3) the Pb atoms occupy two independent sites: Pb1 and Pb2. The coordinations of both Pb1 and Pb2 have the form of a distorted tricapped trigonal prism, if the closest As atom is included in the coordination of Pb2. Pb1 is coordinated by 6 S atoms (2.76–3.64 Å) and 3 I(Cl) atoms (3.35–3.57 Å), Pb2 by 6 S (2.91–3.45 Å) and 2 I(Cl) atoms (3.05–3.45 Å). One "missing" vertex in the Pb2 prism is occupied by an As atom (Pb-As distance of 3.35 Å). Such short Pb-As distances in crystal structures are not unusual. In the two representatives from the apatite group, finnemanite (Effenberger and Pertlik 1979) and mimetite (Dai et al. 1991), distances of 3.27 and 3.37 Å respectively are encountered. In sulfosalts, distances of 3.37 Å are found in, e.g., wallisite (Takeuchi et al. 1968), and dufrenoysite (Marumo and Nowacki 1967).

Pb1-Pb2 prisms are paired on bases made up of two S and one I(Cl) atom, and these pairs connect in columns by sharing an S-S edge with the other base for positions with As atoms. The columns extend along **c** and are laterally connected through Pb-S bonds in layers parallel (100). The As atoms are in threefold coordination with S atoms (As-S = 2.24–2.25 Å) occupying the top of a trigonal pyramid with 3 S making a base. AsS$_3$ coordinations are isolated from each other. The characteristics of the As coordination polyhedra as well as those of the Pb atoms are illustrated in Table 8.

As mentioned above, the crystal structure has a layered character with layers parallel to (100). The median plane of the layers coincides with the n-glide planes. The backbone of each layer is formed by straight [010] rows of S1 atoms with an S1-S1 intrarow separation of 1/2 b (Figs. 4a and 4b). Attached to them on both sides of a layer are the Pb1-X and Pb2-S2 rows. The Pb1 atoms are backed by S2 atoms from the other side of the layer,

TABLE 4. Crystal data and summary of parameters describing data collection and refinement for mutnovskite

Crystal data	
Empirical chemical formula	Pb$_{1.99}$(As$_{0.98}$Bi$_{0.02}$)$_{\Sigma1.00}$(S$_{2.98}$Se$_{0.02}$)$_{\Sigma3.00}$(I$_{0.47}$Cl$_{0.46}$Br$_{0.09}$)$_{\Sigma1.02}$
Crystal size (mm)	0.034 × 0.054 × 0.072
Cell setting, space group	Orthorhombic, $Pnma$
a, b, c (Å)	11.543(1), 6.6764(7), 9.359(1)
V (Å^3)	721.3(1)
Z	4
Dx (g/cm^3)	6.177
Data collection	
Radiation	Mo$K\alpha$ (graphite monochromator)
Temperature	293 K
Detector to sample distance	4 cm
Active detection-area	6.25 × 6.25 cm^2
Resolution	512 × 512 pixels
Number of frames	2800
Rotation width per frame	0.2°
Measuring time	60 s
Maximum covered 2θ	56.58° ($d = 0.75$ Å)
Unique reflections	976
Reflections $I > 2\sigma_I$	753
R_{int} before absorption correction	0.1247
R_{int} after absorption correction	0.0692
R_σ	0.042
Range of h, k, l	$-15 \le h \le 15, -8 \le k \le 8, -12 \le l \le 11$
Refinement	
$R[F_o > 4\sigma(F_o)]$	0.0414
R (all data)	0.0563
wR (on F_o^2)	0.0891
wR (all data)	0.0922
Goof	1.25
Number of least squares parameters	41

TABLE 5. Fractional atomic coordinates and anisotropic displacement parameters (Å) for the crystal structure of mutnovskite

Site	x	y	z	U_{11}	U_{22}	U_{33}	U_{23}	U_{13}	U_{12}	U_{eq}
Pb1	0.37509(6)	1/4	0.19184(8)	0.0342(4)	0.0539(5)	0.0347(4)	0	−0.0073(3)	0	0.0409(2)
Pb2	0.17188(7)	3/4	0.21713(9)	0.0363(4)	0.0817(6)	0.0355(5)	0	−0.0052(3)	0	0.0512(3)
As	0.9213(1)	3/4	0.0355(2)	0.0199(7)	0.0358(9)	0.0246(9)	0	−0.0013(6)	0	0.0268(4)
X	0.9544(1)	3/4	0.4017(2)	0.0283(9)	0.046(1)	0.028(1)	0	−0.0017(7)	0	0.0342(6)
S1	0.2969(3)	0.9998(4)	0.4194(4)	0.037(2)	0.026(1)	0.030(2)	0.001(1)	−0.001(1)	0.002(1)	0.0310(6)
S2	0.5985(4)	1/4	0.2968(5)	0.024(2)	0.066(3)	0.022(2)	0	−0.004(2)	0	0.038(1)

TABLE 7. Selected interatomic distances (Å) and angles (°) for mutnovskite

PB1				CN: 9				
	S2	S1	S1	S2	X	X	X	S1	S1
S2	**2.760(5)**	91.7(1)	91.7(1)	157.2(1)	74.9(1)	81.2(1)	81.2(1)	139.4(1)	139.4(1)
S1	4.028(5)	**2.853(3)**	71.7(1)	70.1(1)	142.2(1)	73.5(1)	144.2(1)	128.3(1)	94.7(1)
S1	4.028(5)	3.341(4)	**2.853(3)**	70.1(1)	142.2(1)	144.2(1)	73.5(1)	94.7(1)	128.3(1)
S2	5.838(7)	3.483(5)	3.483(5)	**3.194(5)**	127.8(1)	105.3(1)	105.3(1)	58.5(1)	58.5(1)
X	3.749(5)	5.875(4)	5.875(4)	5.882(5)	**3.354(2)**	69.6(0)	69.6(0)	75.7(1)	75.7(1)
X	4.166(3)	3.887(4)	6.117(3)	5.383(4)	3.955(1)	**3.570(1)**	138.5(1)	113.4(1)	62.6(1)
X	4.166(3)	6.117(3)	3.887(4)	5.383(4)	3.955(1)	6.676(1)	**3.570(1)**	62.6(1)	113.4(1)
S1	6.007(6)	5.849(5)	4.803(5)	3.361(5)	4.294(4)	6.023(3)	3.743(4)	**3.636(4)**	54.6(1)
S1	6.007(6)	4.803(5)	5.849(5)	3.361(5)	4.294(4)	3.743(4)	6.023(3)	3.336(4)	**3.636(4)**

PB2				CN: 8			
	S1	S1	X	S1	S1	X	S2	S2
S1	**2.906(3)**	70.0(1)	92.3(1)	142.5(1)	102.0(1)	74.9(1)	134.6(1)	65.9(1)
S1	3.336(4)	**2.906(3)**	92.3(1)	102.0(1)	142.5(1)	74.9(1)	65.9(1)	134.6(1)
X	4.294(4)	4.294(4)	**3.047(2)**	125.0(1)	125.0(1)	164.3(1)	79.6(1)	79.6(1)
S1	5.849(5)	4.803(5)	5.603(4)	**3.269(4)**	61.5(1)	67.7(1)	60.0(1)	119.3(1)
S1	4.803(5)	5.849(5)	5.603(4)	3.341(4)	**3.269(4)**	67.7(1)	119.3(1)	60.0(1)
X	3.887(4)	3.887(4)	6.431(2)	3.743(4)	3.743(4)	**3.445(2)**	102.7(1)	102.7(1)
S2	5.865(4)	3.483(5)	4.166(3)	3.361(5)	5.796(4)	5.383(4)	**3.446(1)**	151.2(1)
S2	3.483(5)	5.865(4)	4.166(3)	5.796(4)	3.361(5)	5.383(4)	6.676(1)	**3.446(1)**

AS			CN: 3
	S1	S1	S2
S1	**2.241(3)**	96.2(2)	97.0(1)
S1	3.336(4)	**2.241(3)**	97.0(1)
S2	3.361(5)	3.361(5)	**2.245(5)**

Note: The values in diagonals (bold) are the central atom-ligand distances; the bond angles are given in the upper-right triangle and the ligand-ligand distances are given in the lower left.

TABLE 8. Coordination parameters* for the cation sites of mutnovskite

Site	Coordination	$<d>$	d min	d max	Vs	ECC_L	SPH_L	Vp	υ	valence
Pb1	6S+3X	3.3(4)	2.760(5)	3.336(4)	142.935	0.1645	0.9479	67.1(1)	0.0381	2.07
Pb2	6S+2X	3.2(2)	2.906(3)	3.446(1)	140.064	0.0790	0.9458	50.2(1)	0.1731	1.73
As	3S	2.243(3)	2.241(3)	2.245(5)	30.37	0.5852	1	–	–	3.15

Notes: $<d>$ = average bond distance, Vs = volume of the circumscribed sphere, ECC_L = linear eccentricity of the coordination, SPH_L = linear sphericity of the coordination, Vp = volume of the coordination polyhedron, υ = volume distortion.
* The polyhedron parameters for atomic coordinations are defined by Balić-Žunić and Makovicky (1996) and Makovicky and Balić-Žunić (1998). All calculations were done using *IVTON* (Balić-Žunić and Vicković 1996).

while the Pb2 atoms are in the same way backed by X atoms, in accordance with the *n*-glide symmetry of the layer. In this way the Pb atoms reside in a half-cavity formed by 5S +2X (Pb1) or 6S+1X (Pb2). Arsenic atoms "ride" on each S2 atom and are additionally bonded to the two nearest S1 atoms.

The centers of symmetry and 2_1 axes (parallel to **b**) are situated between the layers. These are mutually attached in such a way that the Pb1-X rows from one layer face the Pb2-S2 rows from the adjacent one, mutually displaced so that Pb atoms from one layer face S and X atoms from the other (Fig. 4c). The rows of As atoms from one layer face As rows from the adjacent one, but due to the mutual 1/2 *b* displacement the As lone-electron pairs point into empty interspaces between the As atoms of the adjacent layer. The coordination of Pb1 is completed to CN9 by the bonds made to S2 and X from the neighboring layer, whilst Pb2 forms only one additional bond (to X) and faces the lone-electron pair of As from the adjacent layer. Although there is no short interlayer As-S bond, the structure does not have a well-expressed layer character due to the fact that the shortest Pb-S and Pb-X bonds are interlayer bonds.

The superposition of layers brings together the two Pb1-X rows from adjacent layers, which are surrounded from all sides by the framework of S and Pb2 atoms (Fig. 5). The latter

framework consists of wavy closed-packed layers parallel to (100). Due to the wavy character of these layers the two types of channels running parallel to [010] are formed in the interlayers. In the smaller ones As atoms bonded to S atoms make up the walls of the channel, with the lone-electron pairs of As pointing inside the channel. The bigger ones each host two Pb1-X rows, as shown in Figure 5.

DISCUSSION

Mutnovskite is the first example of a multi-component sulfosalt where halogens (I, Cl, Br) act as essential constituents together with sulfur, lead, and arsenic. The presence of Cl is well known among natural halogen-bearing sulfosalts (ardaite, $Pb_{10}Sb_6S_{17}Cl_4$ = Breskovska et al. 1982; dadsonite, $Pb_{23}Sb_{25}S_{60}Cl$ = Moëlo 1979; pillaite, $Pb_9Sb_{10}S_{23}ClO_{0.5}$ = Orlandi et al. 2001; pellouxite, $(Cu,Ag)_2Pb_{21}Sb_{23}S_{55}ClO$ = Orlandi et al. 2004; vurroite, $Pb_{20}Sn_2(Bi,As)_{22}S_{54}Cl_6$ = Garavelli et al. 2005). Less usual is the presence of minor Br substituting for Cl, which has only been reported in the recently approved halogen-sulfosalt vurroite (Garavelli et al. 2005). The most interesting feature is the presence of iodine in mutnovskite. The occurrence of I together with Cl and Br is quite common among mercury halogen-sulfides of the corderoite-arzakite and capgaronnite-perroudite groups
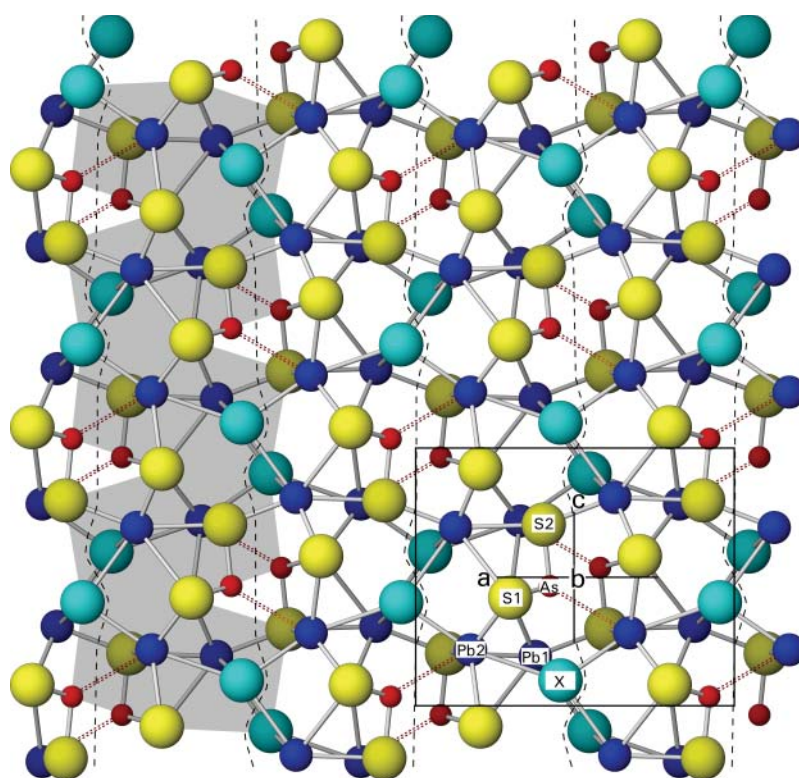
FIGURE 3. The crystal structure of mutnovskite projected on (010). Blue circles: Pb atoms; red circles: As atoms; light blue circles: X sites (I,Cl,Br); yellow circles: S atoms. The unit cell is displaced by $-1/2a$, $-1/2b$, $-1/2c$. Dark dashed lines: limits of layers parallel to (100); red dashed lines: connection from Pb2 to As, which forms the "missing" vertex of the prism. A column of Pb1 and Pb2 trigonal prism is shaded on the left-hand side.
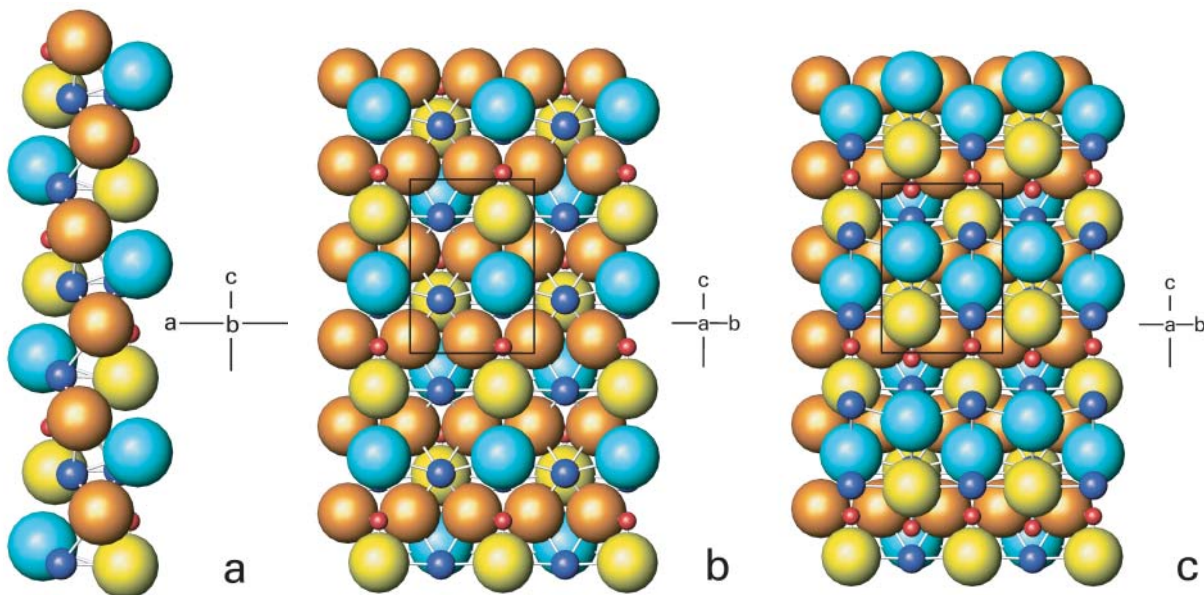

FIGURE 4. The (100) layers in the structure of mutnovskite. The anions are expanded to show the packing. Light blue: X sites (I,Cl,Br); orange: S1 atoms; yellow: S2 atoms; dark-blue: Pb atoms; red: As atoms. (**a**) A view parallel to **b**; (**b**) a layer projected on the (100) plane; (**c**) a superposition of the Pb, As, X, and S2 atoms from the adjacent layer.

(Strunz and Nickel 2001), but certainly it is original among sulfosalts. The presence of iodine in mutnovskite makes this new mineral the first representative of a new mineralogical class: the I-bearing sulfosalts.

According to both the chemical composition and X-ray powder data, the mineral has no analogues among minerals or synthetic compounds. With the exception of the halogen content,

the chemical composition of mutnovskite is close to the mineral tsugaruite, $Pb_4As_2S_7$ (Shimizu et al. 1998). Compositionally, the substitution $2(I,Cl,Br) \rightarrow S$ in tsugaruite would give the formula of mutnovskite $Pb_2AsS_3(I,Cl,Br)$. The strong compositional similarity between the two minerals explains the resemblance in reflectance values and some other physical properties.

In the depositional environment, mutnovskite can be assumed

FIGURE 5. The [010] channels in the crystal structure of mutnovskite. Light blue: X sites (I,Cl,Br); yellow: S atoms; dark-blue: Pb atoms; red: As atoms. (**a**) Pb1- X rows and columns of S atoms along [010]; (**b**) a view along the channels showing the smaller channels which accommodate the lone-electron pairs of As, and the larger ones which host the halogen and Pb1 atoms inside the framework of the wavy close-packed layers of S and Pb2 atoms.

to form according to the reaction: $2AsS + 4PbS + \frac{1}{2}O_2 + 2HX \rightarrow 2Pb_2AsS_3X + H_2O$, with X = I, Cl, Br. This is confirmed by the presence of PbS and As-I-S compounds among sublimates deposited on the inner walls of silica tubes inserted in high-temperature fumarole vents at the Mutnovsky volcano (Zelenski and Bortnikova 2005). The presence of halogens in fluids discharging from fumaroles, as well as their role in the transport of the metals and in the deposition of sulfosalt minerals, has been amply discussed in the literature (Quisefit et al. 1989; Symonds et al. 1987, 1992; Symonds and Reed 1993; Garavelli et al. 1997; Cheynet et al. 2000). In fluids discharging from active volcanoes Cl and Br are the most abundant halogens whilst iodine is rarely found. In volcanic gases from the Mutnovsky volcano the halogen concentrations range as follows: Cl 2800–4800 ppm, Br 3.7–6.00 ppm, and I 0.35–1.7 ppm (Zelenski and Bortnikova 2005). In fumarole environments, especially Cl, but also Br, generally play the double role of carrier for the metals and catalyst in the reactions involving sulfosalts. The use of iodide as a catalyst and as a transport medium during synthesis experiments in the laboratory is well known. Several sulfo-iodides with bismuth and some other metals have been obtained from such syntheses as, e.g., $(Pb_{1-x},Bi_x)Bi_2Cu_2Cu_{2-x}S_5I_2$ (Ohmasa and Mariolacos 1974), $Cu_{4-x} Pb_{1-x}Bi_{2+x}S_5I_2$ (Mariolacos 2004), $Cu_{0.507(5)}Pb_{8.73(9)}Sb_{8.15(8)}I_{1.6}S_{20.0(2)}$ (Kryukova et al. 2005), and $Cu_3Bi_2S_3I_3$ (Balić-Žunić et al. 2005). The presence of iodine in mutnovskite suggests that this element, in addition to chlorine and bromine, could play a significant role in the transport of metals and in the condensation processes of sulfosalts in natural environments with a high partial-pressure of halogens.

Mutnovskite contains traces of Se (up to 1.33 wt%); the presence of this element is ascribed to the high Se content of the fluids discharging from the fumarole vents and it is a common feature of sulfosalts deposited in contemporary epithermal deposits connected to active volcanoes (Borodaev et al. 1998; Vurro et al. 1999; Borodaev et al. 2000, 2001, 2003; Garavelli et al. 2005).

In the depositional environment, mutnovskite occurs commonly interspersed with needle-like crystals of less characterized Pb-Bi-As sulfosalts and occasionally with the Cd-bearing Pb-Bi sulfosalts kudriavite and Cd-cannizzarite.

The sequence of deposition observed in all the samples analyzed (greenockite-kudriavite and Cd-cannizarite-Pb-Bi-As sulfosalts-mutnovskite) suggests a strong relationship between temperature and sulfosalts deposition at the Mutnovsky volcano. At high temperature (480 °C) the most abundant sulfosalt is greenockite, while mutnovskite occurs at quite a low temperature (250 °C). The Cd-bearing sulfosalts kudriavite and Cd-cannizzarite and Pb-Bi-As sulfosalts occur at intermediate temperature values. This evidence is in contrast with the condition of deposition observed in the actual epithermal deposit of the La Fossa crater of Vulcano, Aeolian Islands, Italy (Garavelli et al. 2005; Borodaev et al. 2003). This latter deposit is characterized by a sulfosalt assemblage which is very similar to that occurring at the Mutnovsky volcano, but no relevant paragenetic sequence of deposition could be observed. The discrepancy between the two fumarole deposits could be explained with a more stable chemical composition, temperature, and flux rate of the fumarole fluids discharging from the Mutnovsky volcano with respect to the fluids emitted from Vulcano fumaroles, the latter which have been found to change instantaneously (Borodaev et al. 2003).

REFERENCES CITED

Balić-Žunić, T. and Makovicky, E. (1996) Determination of the centroid or "the best centre" of a coordination polyhedron. Acta Crystallographica, B52, 78–81.

Balić-Žunić, T. and Vicković, I. (1996) IVTON— Program for the calculation of geometrical aspects of crystal structures and some crystal chemical applications. Journal of Applied Crystallography, 29, 305–306.

Balić-Žunić, T., Mariolacos, K., and Makovicky, E. (2005) Crystal structure of a synthetic halogen-sulfosalt, $Cu_3Bi_2S_3I_3$. Acta Crystallographica, B61, 239–245.

Borodaev, Y.S., Garavelli, A., Kuzmina, O.V., Mozgova, N.N., Organova, N.I., Trubkin, N.V., and Vurro, F. (1998) Rare sulfosalts from Vulcano, Aeolian Islands, Italy. I. Se-bearing kirkiite, $Pb_{10}(Bi,As)_6(S,Se)_{19}$. Canadian Mineralogist, 36, 1105–1114..

Borodaev, Y.S., Garavelli, A., Garbarino, C., Grillo, S.M., Mozgova, N.N., Organova, N.I., Trubkin, N.V., and Vurro, F. (2000) Rare sulfosalts from Vulcano, Aelian Islands, Italy. III. Wittite and Cannizzarite. Canadian Mineralogist, 38, 23–34.

Borodaev, Y.S., Garavelli, A., Garbarino, C., Grillo, S.M., Mozgova, N.N., Uspenskaya, T.Y., and Vurro, F. (2001) Rare sulfosalts from Vulcano, Aeolian Islands, Italy. IV. Lillianite. Canadian Mineralogist, 39, 1383–1396.

Borodaev, Y.S., Garavelli, A., Garbarino, C., Grillo, S.M., Mozgova, N.N., Paar W.H., Topa, D., and Vurro, F. (2003) Rare sulfosalts from Vulcano, Aeolian Islands, Italy. V. Selenian Heyrovskýite. Canadian Mineralogist, 41, 429–440.

Breskovska, V.V., Mozgova, N.N., Bortnikov, N.S., Gorshov, A.I., and Tsepin, A.I. (1982) Ardaite—a new lead-antimony chlorosulphosalt. Mineralogical Magazine, 46, 357–361.

Bruker AXS (1997a) SAINT Plus, Version 6.02/NT—Bruker Analytical X-ray Systems, Inc. Madison, Wisconsin 53719, U.S.A.

——— (1997b) SHELXTL, Version 5.1. — Bruker Analytical X-ray Systems, Inc. Madison, Wisconsin 53719, U.S.A.

——— (1998) SMART, Version 5.1. — Bruker Analytical X-ray Systems, Inc. Madison, Wisconsin 53719, U.S.A.

Cheynet, B., Dall'Aglio, M., Garavelli, A., Grasso, M.F., and Vurro, F. (2000) Trace elements from fumaroles at Vulcano Island (Italy): rates of transport and a thermochemical model. Journal of Volcanology and Geothermal Research, 95, 273–283.

Dai, Y.-S., Hughes, J.M., and Moore, P.B. (1991) The crystal structures of mimetite and clinomimetite, $Pb_5(AsO_4)_3Cl$. Canadian Mineralogist, 29, 369–376.

Effenberger, H. and Pertlik, F. (1979) Die Kristalstruktur des Finnemanits, $Pb_5Cl(AsO_3)_3$ mit einem Vergleich zum Strukturtyp des Chlorapatits, $Ca_5Cl(PO_4)_3$. Tschermaks Mineralogische und Petrographische Mitteilungen, 26, 95–107.

Garavelli, A., Laviano, R., and Vurro, F. (1997) Sublimate deposition from hydrothermal fluids at the Fossa crater—Vulcano, Italy. European Journal of Mineralogy, 9, 423–432.

Garavelli, A., Mozgova, N.N., Orlandi, P., Bonaccorsi, E., Pinto, D., Moelo, Y., and Borodaev, Y. (2005) Rare sulfosalts from Vulcano, Aeolian Islands, Italy. VI. Vurroite, $Pb_{20}Sn_2(Bi,As)_{22}S_{54}Cl_6$, a new mineral species. Canadian Mineralogist, 43, 703–711.

Ibers, J.A. and Hamilton, W.C., Eds. (1974) International Tables for X-ray Crystallography, vol. IV, 366 p. Kynock, Dordrecht, The Netherlands.

Kryukova, G N., Heuer, M., Wagner, G., Doering, T., and Bente, K. (2005) Synthetic $Cu_{0.507(5)}Pb_{8.73(9)}Sb_{8.15(8)}I_{1.6}S_{20.0(2)}$ nanowires. Journal of Solid State Chemistry, 178, 376–381.

Makovicky, E. and Balić-Žunić, T. (1998): New measure of distortion for coordination polyhedra. Acta Crystallographica, B54, 766–773.

Mariolacos, K. (2004) Single crystal synthesis of higher-order sulfohalogenides in the temperature gradient: $Bi_{19}S_{27}Br_3$, $Bi_2Cu_3S_4Br$, $Pb_{1-x}Bi_{2+x}Cu_{4-x}S_5I_2$. Material Research Bulletin, 39, 591–598.

Marumo, F. and Nowacki, W. (1967) The crystal structure of dufrenoysite, $Pb_{16}As_{16}S_{40}$. Zeitschrift für Kristallographie, 124, 409–419.

Moëlo, Y. (1979) Quaternary compounds in the system Pb-Sb-S-Cl: dadsonite and synthetic phases. Canadian Mineralogist, 17, 595–600.

Ohmasa, M. and Mariolacos, K. (1974) The crystal structure of $(Pb_{1-x}Bi_x)Bi_2Cu_2Cu_{2-x}S_5I_2$ (x = 0.88). Acta Crystallographica, B30, 2640–2643.

Orlandi, P., Moëlo, Y., Meerschaut, A., and Palvadeau, P. (2001) Lead-antimony sulfosalts from Tuscany (Italy). III. Pillaite, $Pb_9Sb_{10}S_{23}ClO_{0.5}$, a new Pb-Sb chloro-sulfosalt, from Buca della Vena mine. European Journal of Mineralogy, 13, 605–610.

Orlandi, P., Moëlo, Y., Meerschaut, A., Palvadeau, P., and Léone, P. (2004) Lead-antimony sulfosalts from Tuscany (Italy). VI. Pellouxite, ~ $(Cu,Ag)_2Pb_{21}Sb_{23}S_{55}ClO$, a new oxy-chloro-sulfosalt, from Buca della Vena mine, Apuan Alps. European Journal of Mineralogy, 16, 839–844.

Quisefit, J.P., Toutain, J.P., Bergametti, G., Javoy, M., Cheynet, B., and Person, A. (1989) Evolution versus cooling of gaseous volcanic emissions from Momotombo Volcano, Nicaragua: Thermochemical model and observations. Geochimica and Cosmochimica Acta, 53, 2591–2608.

Sheldrick, G.F. (1997a) SHELXS-97. A program for automatic solution of crystal structures. University of Göttingen, Germany.

——— (1997b) SHELXL-97. A program for crystal structure refinement. University of Göttingen, Germany.

Shimizu, M., Miyawaki, R., Kato, A., Matsubara, S., Matsuyama, F., and Kiyota, K. (1998) Tsugaruite, $Pb_4As_2S_7$, a new mineral species from the Yunosawa mine, Aomori Prefecture, Japan. Mineralogical Magazine, 62, 793–799.

Strunz, H. and Nickel, E.H. (2001) Strunz Mineralogical Tables. Chemical-Structural Mineral Classification System, 9th ed., 870 p. Schweizerbart Edit., Stuttgart, Germany.

Symonds, R.B. and Reed, M.H. (1993) Calculation of multicomponent chemical equilibria in gas-solid-liquid systems: calculation methods, thermochemical data and applications to studies of high-temperature volcanic gases with examples from Mount St. Helens. American Journal of Science, 293, 758–864.

Symonds, R.B., Rose, W.I., Reed, M.H., Lichte, F.E., and Finnegan, D.L. (1987) Volatilization, transport and sublimation of metallic and non-metallic elements in high- temperature gases at Merapi Volcano, Indonesia. Geochimica et Cosmochimica Acta, 51, 2083–2101.

Symonds, R.B., Reed, M.H., and Rose, W.I. (1992) Origin, speciation and fluxes of trace-element gases at Augustine volcano, Alaska: Insights into magma degassing and fumarolic processes. Geochimica et Cosmochimica Acta, 56, 633–657.

Takeuchi, Y., Ohmasa, M., and Nowacki, W. (1968) The crystal structure of wallisite, $PbTlCuAs_2S_5$, the Cu-analoge of hatchite, $PbTlAgAs_2S_5$. Zeitschrift für Kristallographie, 127, 349–365.

Vurro, F., Garavelli, A., Garbarino, C., Moëlo, Y., and Borodaev, Y.S. (1999) Rare sulfosalts from Vulcano, Aeolian Islands, Italy. II. Mozgovaite $PbBi_4(S,Se)_7$, a new mineral species. Canadian Mineralogist, 37, 1499–1506.

Zelenski, M.E. and Bortnikova, S. (2005) Sublimate speciation at Mutnovsky volcano, Kamchatka. European Journal of Mineralogy, 17, 107–118.